20th Australasian Fluid Mechanics Conference
Perth, Australia
5-8 December 2016

# Complementary CFD Study of Generic Submarine Model Tests in a Cavitation Tunnel

**Chris L. Ellis[1,2], David B. Clarke[1], Daniel Butler[1,2], Paul Brandner[2]**

[1]Maritime Division, Defence Science and Technology Group, Fishermans Bend, Victoria, 3207, Australia

[2]Australian Maritime College,
University of Tasmania, Launceston, Tasmania, 7250, Australia

## Abstract

Experimental and computational studies were conducted on the widely studied SUBOFF submarine model enabling the benchmarking of the Australian Maritime College (AMC) cavitation tunnel for submarine model testing. This paper describes the Computational Fluid Dynamics (CFD) used in conjunction with the SUBOFF experiments in this study. The CFD was used to determine blockage corrections and to provide insight into the development of flow structures that are observed in the wake measurements.

The blockage correction was determined using computational domains representative of the test environment and an additional enlarged domain with a low blockage ratio. The simulations of the submarine hull in the former compared well with the uncorrected test measurements. This high level of agreement provides confidence in using the results from the simulations to correct for blockage.

These corrections allow the results obtained in the AMC cavitation tunnel to be compared with results obtained in other test facilities (e.g. the David Taylor Research Centre); which showed a high level of agreement.

## Introduction

The geometric parameters of a submarine's hullform can have a significant influence on its manoeuvrability, drag and wake. Therefore, it is important to understand the role the nose shape, length/diameter ratio, tail cone angles and casing design (Figure 1) have on a submarine's performance as early in the design process as possible.

Experimental test programs and Computational Fluid Dynamics (CFD) studies play a critical and complementary role in obtaining an understanding of the flow around submarines. While there are many cases where CFD can provide results in a more cost effective and timely manner, the judicious use of experimental testing is necessary to provide verification for a subset of the simulated cases. Conversely CFD can be used in support of the experimental program as well. Once a comparison of the experimental and CFD results provide confidence in the computational results, the CFD may be used to correct for a number of aspects in the experimental setup, including blockage.

DST Group investigated the Defence Advanced Research Project Agency (DARPA) SUBOFF model generic hullform [3] shown in Figure 1 in the Australian Maritime College (AMC) cavitation tunnel This model is representative of a nuclear submarine and has been widely studied using experimental and computational techniques. The investigation of the SUBOFF model allowed benchmarking of the AMC cavitation tunnel for submarine hullform testing. This paper describes the CFD used to support the experimental investigations of the SUBOFF submarine hullform that were performed in the AMC cavitation tunnel [1,2]. The CFD simulations, verified in comparison with the experimental results, were used for blockage correction.

## Method

### Models

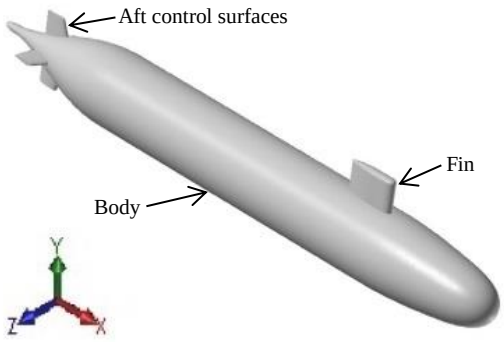


Figure 1. Fully appended SUBOFF generic nuclear submarine hullform.

The SUBOFF model has been tested in a number of configurations, including the unappended axisymmetric body and with a variety of appendages [6]. In this set of experiments and CFD simulations, only the unappended axisymmetric body was studied. As the CFD simulations were conducted to compliment the measurements, the support foils used to mount the physical model in the AMC cavitation tunnel test section were included in the simulations. The SUBOFF model used in the measurements and computations has a length, $L$, of 1.543 m with a maximum radius, $r_{max}$, of 0.090 m (diameter of 0.180 m). The two NACA0016 profile support foils (Figure 2) have a root chord of 0.140 m (0.091 $L$) and are spaced 0.450 m (0.291 $L$) between centres. The support foils have a taper ratio of 0.715 with the taper ending approximately 0.040 m (0.44 $r_{max}$) before entering the hull. The distance from the test section ceiling to the model centre line is approximately 0.29 m (3.2 $r_{max}$).

### Computational Domain and Mesh

To determine the influence of blockage two computational domains, including the generic submarine model and supports, were created (shown in Figure 2). These were the:

- domain representing the environment due to the AMC cavitation tunnel test section with a solid blockage of ≈8%; and
- a low blockage domain with a solid blockage of 0.49%.

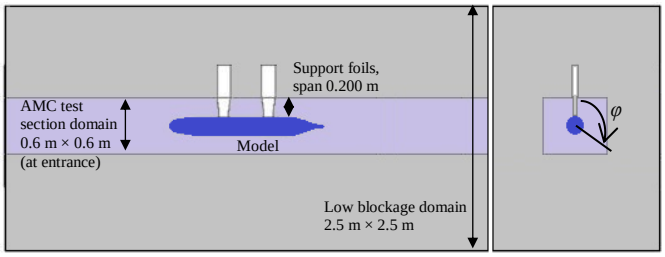


*Figure 2. The layout of the SUBOFF model within the AMC test section domain and the low blockage domain. The purple shaded area denotes the AMC test section domain, the grey shaded area denotes the low blockage domain and the blue denotes the submarine model. Note: diagram not to scale.*

The outer extent of the smaller domain (referred to as the AMC test section domain) in the non-streamwise directions was chosen to match that of the AMC cavitation tunnel's test section. The latter has a 0.600 m x 0.600 m (6.667 $r_{max}$) cross section at the entrance and is 0.620 m (6.889 $r_{max}$) high at the exit with a length of 2.60 m (1.685 $L$). The change in height occurs due to a slope on the cavitation tunnel test section floor of 0.44° and compensates for the boundary layer growth on the walls of the test section. This computational domain representing the test section was lengthened 2.376 m (1.542 $L$) upstream and 2.685 m (1.737 $L$) downstream to minimise non-physical inlet and exit behaviour.

The low blockage computational domain for the model extends the width and height of the domain to 2.50 m (27.78 $r_{max}$). This computational domain is also extended 2.38 m (1.542 $L$) upstream and 2.68 m (1.737 $L$) downstream of the model's nose and tail, respectively. The significant reduction in blockage due to the increased cross section allows for the examination of blockage effects. The support foils were extended into the low blockage domain, but were set as slip walls outside of the AMC test section domain. The location of the truncation of the support foils a significant distance from the hull minimised any effects due to their termination on the flow around the hull.

Structured meshes were created for computing the flow around the SUBOFF hull. The streamlined supports are included in these meshes. The finest mesh for the SUBOFF hull in the cavitation tunnel test section is comprised of 68 million cells, while the low blockage domain contained 123 million cells.

### Simulation Parameters

The ANSYS Fluent solver with the realisable $k$-$\varepsilon$ turbulence model and an enhanced wall function were employed for these simulations. A basic, two-equation model was chosen due to the simple, attached nature of the flow and to reduce computational overhead. The realisable $k$-$\varepsilon$ model was selected as it is reported to be the most suitable of the $k$-$\varepsilon$ turbulence models for handling streamline curvature, separation and vorticity [4]. The realisable $k$-$\varepsilon$ model has also demonstrated good performance in previous compatible studies [2,5].

A second order upwind scheme was used for spatial discretisation of the continuity, momentum and turbulence equations. A least squares cell-based method was used for evaluation of the gradients and derivatives. The SIMPLEC method (with skewness correction) was utilised for the pressure-velocity coupling.

### Inlet Conditions and Boundary Conditions

The uniform inlet boundary velocity, $U_{inlet}$, used for all the domains was set so the Reynolds number based on the hull length for the SUBOFF model was $12\times10^6$. The use of a slip wall on the extended inlet of the domain representing the cavitation tunnel test section avoided the development of an excessively thick boundary layer at the start of the cavitation tunnel test section. The boundary layer however develops once the flow enters the portion of the domain representing the cavitation cavitation tunnel test section wall boundary layer flow should have negligible influence on the flow in the central region of the domain where the submarine geometry is placed. The inlet turbulence intensity was set at 0.5%, which is consistent with the inlet values at the start of the cavitation tunnel test section [1]. The turbulent viscosity ratio at the inlet was set to 10.

The height of the first off-wall cell was set to correspond to a $y^+$ value of approximately 30 across the hull. Due to the lack of flow separation a wall function was selected for the CFD simulations.

### Grid Resolution

The grid sensitivity check was conducted for the SUBOFF mesh using the domain representing the AMC cavitation tunnel test section. Three lower resolution meshes were created, containing 17.9, 25.3 and 37.4 million cells. This represents a reduction in the number of cells by 73.6%, 62.8% and 45%, respectively.

The percentage change in the $x$ velocity component, $\Delta u_{res}$, for the coarsest ($u_{low}$), second coarsest ($u_{ml}$), and second finest ($u_{mh}$) meshes compared to the higher ($u_{hi}$) resolution mesh were calculated as per equation 1.

$$\Delta u_{res} = 100 \times \frac{u_{hi}-u_{low}}{u_{hi}}, 100 \times \frac{u_{hi}-u_{ml}}{u_{hi}}, 100 \times \frac{u_{hi}-u_{mh}}{u_{hi}}, \quad (1)$$

Figure 3 shows the mean $x$-direction velocity, $u$, along a radial line from the centre of the hull at $\varphi = 135°$ and $x = 0.7\ L$. $\varphi$ is the azimuthal angle from the support foils (Figure 2) and $x = 0$ is located at the model nose. There is a negligible difference between the results from the finest and coarser meshes except in the first few cells from the hull surface. The largest percentage change in the velocity, $\Delta u_{res}$, for the coarsest, second coarsest and second finest mesh are 15.23%, 6.97% and 2.36%, respectively, (not shown on the graph) and occurs at the first point off the surface of the hull. For the remaining cells $\Delta u_{res}$ for both the second coarsest and second finest mesh is less than 0.02%. The coarsest mesh demonstrates $\Delta u_{res}$ for the majority of the remaining cells of less than 0.08%. The change in drag determined between these four meshes was negligible. The difference between the coarsest, second coarsest and second finest compared to the finest mesh is 0.0187%, 0.0192% and 0.104% respectively.

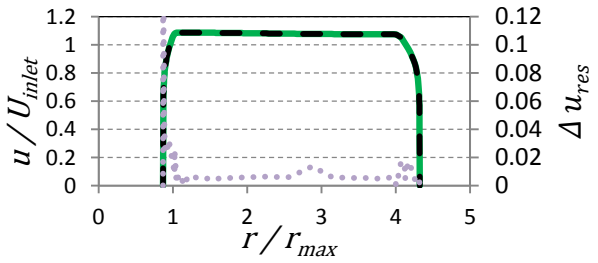


*Figure 3. Normalised mean velocity as a function of normalised radius for the two finest meshes, along a line 135° from the spanwise direction of the support foils for the SUBOFF hullform at a longitudinal position of $x = 0.7\ L$ along the model. Results from the high resolution mesh, $u_{hi}$, are shown by the green line and results from the second finest resolution mesh, $u_{mh}$, by the black dashed line. The purple dots represent $\Delta u_{res}$ for the second finest mesh.*

## Results

### Test Section Flow Velocity

The blockage effects velocity ratio $\left(\frac{(u_{TS})_{max}}{(u_{LB})_{max}}\right)$ for the SUBOFF model against streamwise location is shown in Figure 4. $(u_{TS})_{max}$ is the maximum velocity, determined from the AMC

test section domain simulation, along a given line normal to the hull centre line at a value of $x$ and $\varphi$ corresponding to each measurement position. $(u_{LB})_{max}$ is the corresponding maximum velocity determined from the low blockage domain simulation. The presence of the SUBOFF model within the AMC cavitation tunnel test section represents a solid blockage ratio of approximately 8.1% [1]. This blockage results in an increase of velocity ratio by 6.53%. The velocity ratio is used in the blockage correction of skin friction (equation 3) where it is determined at each value of $x$ and $\varphi$ corresponding to the skin friction measurement location.

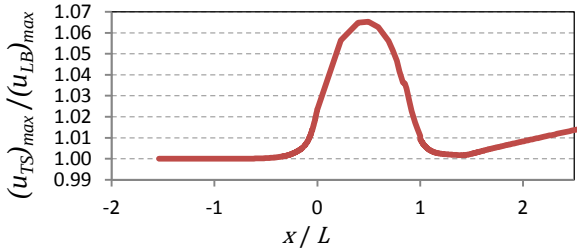


Figure 4. The maximum velocity ratio of the AMC test section domain, $u_{TS}$, to the low blockage domain, $u_{LB}$, for the SUBOFF hullform. The horizontal axis is normalised by the length of the SUBOFF model, where $x = 0$ is at the tip of the model nose.

## Surface Pressure

Surface pressure coefficient, $C_p$, distributions on the surface of the SUBOFF hullform determined from measurements and CFD simulations are shown in Figure 5. The calculated $C_p$ distribution determined from the AMC test section domain simulation compare closely to the uncorrected measurements obtained in the AMC cavitation tunnel [1]. The success of the CFD calculation for the AMC tunnel domain provides confidence to use the CFD simulations to perform a correction to allow for the confines of the test section. The calculated $C_p$ distribution from the low blockage domain simulation corresponds well to the measured $C_p$ distribution from the David Taylor Research Centre (DTRC) Anechoic Flow Facility [3] and the corrected $C_p$ distribution measurements from the AMC cavitation tunnel.

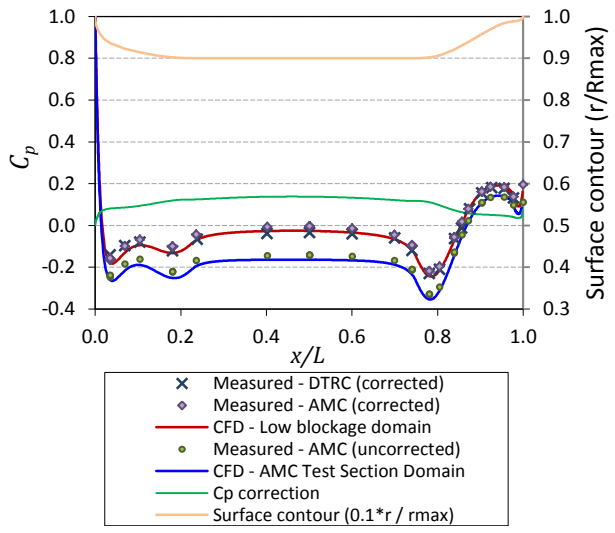


Figure 5. Surface pressure coefficient ($Cp$) distribution for the SUBOFF hullform: AMC test section domain (CFD), low blockage domain (CFD), DTRC [3] (measured, uncertainty = 0.015) and AMC [1] (measured, uncertainty 0.007) at Re = $12\times10^6$.

The blockage corrections for the surface pressure coefficient distribution, $\Delta C_p$, are determined from the difference in the calculated surface pressure coefficient distribution between the domain representing the model in the AMC cavitation tunnel test section, $C_{p,TS}$, and the low blockage domain, $C_{p,LB}$[1]. This is shown in equation (2), where the correction is a function of the surface position.

$$\Delta C_p = C_{p,LB} - C_{p,TS} \qquad (2)$$

The influence of blockage on the surface pressure distribution is demonstrated by the reduced pressure around the model in the measured [1] and computed results in the AMC test section domain.

## Skin Friction

In Figure 6 a comparison of skin friction results determined from measurement and computation for the SUBOFF hullform is shown. The results from the two CFD simulations are compared against experimental data from the DTRC SUBOFF measurements [3] and the results obtained in the AMC cavitation tunnel [1]. When comparing the two CFD results, it is seen that the CFD simulation within the AMC test section domain exhibits a higher skin friction along the majority of the length of the model. This is due to the additional flow acceleration around the model resulting from blockage.

The skin friction coefficient distribution determined from measurements on the SUBOFF model in the AMC cavitation tunnel test section and the CFD results for the SUBOFF geometry in the AMC cavitation tunnel test section show good agreement [1].

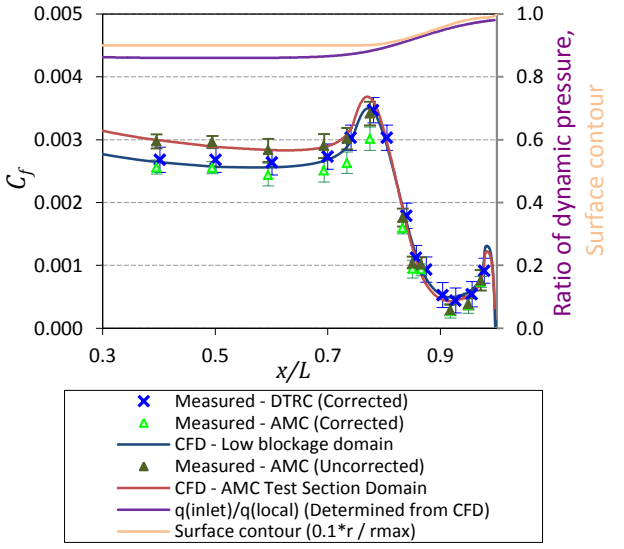


Figure 6. Skin friction results contrasting the CFD calculations to the original DTRC SUBOFF measurements [3] and the AMC experimental data [1] at Re=$12\times10^6$. The surface contour of the SUBOFF hullform and the ratio of dynamic pressure, $q(inlet)/q(local)$, is also included for reference.

Despite the successful calculation of skin friction shown in Figure 6, it is common for RANS CFD simulations to do a less satisfactory job calculating the skin friction coefficient than that achieved in this simulation. The blockage correction applied to the skin friction coefficient determined from the cavitation tunnel measurements was based on the ratio of the calculated maximum dynamic pressure both in the test section and the low blockage domain. The maximum dynamic pressure was selected as the basis for the correction as it is strongly coupled to the skin friction and will generally be accurately calculated by CFD. The correction is a function of surface position. The corrected skin friction, $C_f$, is given thus by,

$$C_f = \left(\frac{\tau_w}{0.5\rho U_\infty^2}\right)_{measured} \left(\frac{(u_{LB})_{max}}{(u_{TS})_{max}}\right)^2_{CFD} \quad (3)$$

where $\tau_w$ is the measured wall shear stress.

A comparison of the corrected skin friction coefficient distributions around SUBOFF is shown in Figure 6. The corrected results from measurements in the AMC cavitation tunnel and the DTRC show good agreement for the majority of measurement positions.

### Boundary layer velocities

Boundary layer velocity profiles are shown in Figure 7 for two of the four locations measured at the aft of the hull. The measurements in the AMC test section were taken normal to the hull's axis and at $\varphi = 135°$ (shown in Figure 2). This allowed the probe to travel further out from the hull. The measurements were corrected by applying a velocity factor for each measurement position, as in equation (4). This correction accounts for the change in boundary layer profile caused by the interaction of the blockage effect and the hull's natural pressure gradient. The corrected AMC measurements are in good agreement with both the DTRC measurements and the low blockage domain CFD.

$$\frac{u_{x,i}}{U} = \left(\frac{u_{x,i}}{U_{inlet}}\right)_{measured} \left(\frac{u_{x,i,\mathrm{LB}}}{u_{x,i,TS}}\right)_{CFD} \quad (4)$$

Where $u_i$ is the velocity at the $i^{\text{th}}$ measurement position.

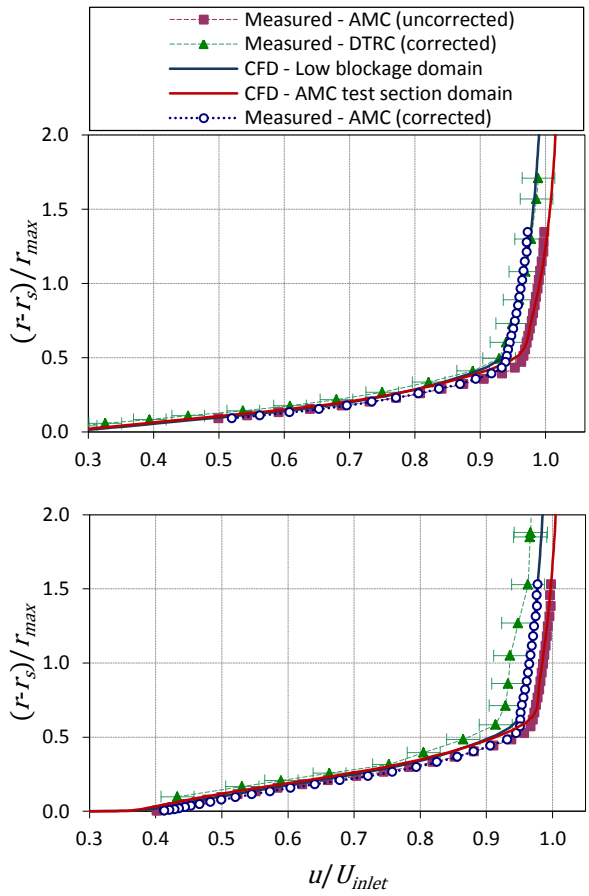


Figure 7. Boundary layer velocities for $x/L$=0.927 (top) and 0.978 (bottom). AMC test section domain (CFD), low blockage domain (CFD), DTRC [3] (measured) and AMC [1] (measured, uncertainty 0.014) at Re=12×10$^6$. Where $r_s$ is the local hull radius and ($r$-$r_s$) is the distance from the surface at $\varphi = 135°$.

## Conclusions

The CFD simulations of the SUBOFF submarine model in the AMC test section domain compare well with the experimental data obtained in the AMC tunnel. The calculation of flow around the submarine hullform is assisted as the flow around the body is attached in this study. The success of the CFD simulations of the AMC test section domain provides confidence in the results obtained in the low blockage domain as these calculations are fundamentally similar. The combination of the CFD simulations in the AMC test section domain and the low blockage domain provides the required information to calculate blockage corrections. These corrections allow the results obtained in the AMC cavitation tunnel to be compared with results obtained in other test facilities that in most cases will also have been corrected for blockage.

With the corrections provided by the CFD, the AMC experimental results compare well with results obtained from the DTRC SUBOFF experiments [3]. In addition, the low blockage domain CFD simulation results also compare well with the data from the original experiments conducted to characterise the DARPA SUBOFF model [3].

The CFD simulations combined with the correction techniques have provided accurate blockage corrections for a relatively large solid blockage ratio in the AMC cavitation tunnel. This work supported the benchmarking of the AMC cavitation tunnel for submarine model testing.

## References


[1] Butler, D., Clarke, D.B., Ellis, C.L., Brandner, P. Benchmarking the AMC cavitation tunnel for hydrodynamic measurements on submarine models with CFD determined blockage corrections, *DSTO-TR-TBC*, Melbourne, Vic., Defence Science and Technology Group (Australia), 2016.

[2] Clarke, D.B., Experimental and computational investigation of flow about low aspect ratio ellipsoids at transcritical Reynolds numbers. [PhD Thesis] Launceston, University of Tasmania, Australia, 2009.

[3] Groves N.C., Huang T.T. and Chang M.S., Geometric characteristics of DARPA SUBOFF models, *DTRC.SHD-1298-01*, 1989.

[4] Kim. S. E., Choudhury, D. and Patel, B., Computations of complex turbulent flows using the commercial code Fluent. *Modelling complex turbulent flows*, M.D. Salas et al., eds., Kluwer Academic Publishers, 1999 pp. 259-276.

[5] Lacasse, D., Turgeon, E., and Pelletier, D., On the judicious use of the k–ε model, wall functions and adaptivity, *International Journal of Thermal Sciences*, 2004, 43.10: 925-938.

[6] Liu, H. and Huang, T. T., Summary of DARPA Suboff Experimental Program Data, *Naval Surface Warfare Center, Carderock Division*, 1998.